$$M[d\phi(t)/dt]+\phi(t)+1 = 1-[d\tau(t)/dt] \quad (1)$$

and

$$\int_{t-\tau(t)}^{t} g[\phi(t')]\,dt' = A(\text{constant}) \quad (2)$$

In the above equations, ϕ is the nondimensionalized pressure in the rocket motor

$$\phi = [p(t)-\bar{p}]/\bar{p} \quad (3)$$

where bar denotes the mean value; M is the ratio of the mass of the hot air in the rocket motor to the mean mass flow rate; $g(\phi)$ is a positive monotonically increasing function of ϕ representing the rate of heat transfer from the combustion gas to the liquid propellant; and τ is the variable time lag.

Equations (1) and (2) can be combined to give

$$M\frac{d\phi(t)}{dt} + \phi(t) = \frac{g[\phi(t)]-g\{\phi[t-\tau(t)]\}}{g[\phi(t)-\tau(t)]} \quad (4)$$

It was shown that, if the equation is linearized, a necessary condition for unconditional stability, that is, stability for any value of τ, is given by

$$\left.\frac{dg(\phi)}{d\phi}\right|_{\phi=0} < \tfrac{1}{2}g(0) \quad (5)$$

This condition is sufficient only for infinitesimally small disturbances. In what follows, a sufficient condition for finite disturbances is derived.

It can be seen that the steady-state solution of Eq. (4) is $\phi = 0$. Let us consider a case where the system is disturbed for $t < 0$ such that

$$-1 < -\phi_m \leqq \phi(t) \leqq \phi_m, \quad \text{for} \quad t \leqq 0 \quad (6)$$

Regarding the behavior of $\phi(t)$ for large t, there are three possibilities; namely; 1) $\dot{\phi} \geqq 0$, for all t greater than some T_1, 2) $\dot{\phi} \leqq 0$, for all t greater than some T_2, or 3) ϕ is an oscillating function.

If the first condition is satisfied, then it is seen from Eq. (4) that

$$g[\phi(t-\tau)] \leqq \{g[\phi(t)]/[1+\phi(t)]\} \quad t > T_1 \quad (7)$$

If $g(\phi)$ is such that

$$(d/d\phi)[g(\phi)/(1+\phi)] \leqq 0, \quad \text{for} \quad |\phi| < \phi_m \quad (8)$$

then the right-hand side of the equality is a decreasing function of time whereas the left hand is an increasing function. They must, therefore, tend to their common limit, $g(0)$.

If the second condition is satisfied, then from Eq. (4)

$$g[\phi(t-\tau)] \geqq \{g[\phi(t)]/[1+\phi(t)]\}, \quad \text{if} \quad \phi > -1 \quad (9)$$

and

$$g[\phi(t-\tau)] \leqq \{g[\phi(t)]/[1+\phi(t)]\}, \quad \text{if} \quad \phi < -1 \quad (10)$$

Since $g > 0$, clearly, $\phi > -1$. This is expected because, $\phi < -1$ means negative pressure. If condition (8) is satisfied, the left-hand side of inequality (9) is a decreasing function of time, whereas the right-hand side is an increasing function. Hence, ϕ must tend to zero as before.

Suppose, ϕ is an oscillating function. Let the first local maxima or minima of $\phi(t)$ for $t > 0$, occur at $t = t_1$. Then for $0 \leqq t \leqq t_1$, we have $\phi_2(t) \leqq \phi(t) \leqq \phi_1(t)$, where ϕ_1 and ϕ_2 are defined as follows:

$$M(d\phi_1/dt)+\phi_1 = \{[\![g[\phi_1(t)]-g(-\phi_m)]\!]/g(-\phi_m)\} \quad (11)$$

and

$$M(d\phi_2/dt)+\phi_2 = \{[\![g[\phi_2(t)]-g(g_m)]\!]/g(\phi_m)\} \quad (12)$$

with $\phi(0) = \phi_1(0) = \phi_2(0)$. The steady-state solutions of Eqs. (11) and (12), ϕ_n and $+\phi_k$, respectively, are given by

$$[g(\phi_n)/(1+\phi_n)] = g(-\phi_m) \quad (13)$$

$$[g(\phi_k)/(1+\phi_k)] = g(\phi_m) \quad (14)$$

Let $f(\phi)$ be a continuous monotonically increasing function which satisfies the relations

$$[f(\phi)/(1+\phi)] = f(-\phi), \quad \text{for} \quad \phi \geqq 0 \quad (15)$$

$$f(0) = g(0) \quad (16)$$

Let g be bounded by f and $g(0)$, such that

$$|g(\phi)-g(0)| \leqq |f(k\phi)-g(0)| \quad (17)$$

where $k < 1$. Then we find

$$[g(\phi)/(1+k\phi)] < g(-\phi), \quad \text{for} \quad \phi > 0 \quad (18)$$

and

$$[g(\phi)/(1+k\phi)] > g(-\phi), \quad \text{for} \quad \phi < 0 \quad (19)$$

Under these conditions Eqs. (13) and (14) imply that

$$|\phi_k| < \phi_m k; \qquad |\phi_n| < \phi_m k \quad (20)$$

Hence

$$|\phi(t_1)| < k\phi_m \quad (21)$$

Similarly, at the next maxima or minima point, $t = t_2$, we have

$$|\phi(t_2)| < k^2\phi_m \quad (22)$$

Hence, ϕ must tend to zero.

In case $g(\phi)$ is linear over the range, $-\phi_m$ to ϕ_m, the sufficient condition reduces to

$$(dg/d\phi) < [g(0)k/(2+\phi_m k)] \quad (23)$$

For infinitesimal disturbances, the condition is given by

$$\left.\frac{dg}{d\phi}\right|_{0^+} + \left.\frac{dg}{d\phi}\right|_{0^-} < g(0)k \quad (24)$$

which reduces to condition (5) given by Crocco, if $dg/d\phi$ is continuous at $\phi = 0$.

Amplitude of Oscillations

Consider a system where $g(\phi)$ is a monotonically increasing function and that $[g/(1+\phi)]$ is a monotonically decreasing function. Let $dg/d\phi$ at $\phi = 0$ be sufficiently large so that the system is unstable.

Suppose there is a function $f(\phi)$, as defined by Eq. (15), such that

$$|g(\phi)-g(0)| \leqq |f(q\phi)-g(0)|, \quad \text{for} \quad \phi > -1 \quad (25)$$

where $q > 1$, and

$$|g(\phi)-g(0)| \leqq |f(k\phi)-g(0)|, \quad \text{for} \quad \phi_a \leqq \phi \leqq \phi_b \quad (26)$$

where $k < 1$. In order words, condition (17) is satisfied for a range $\phi_a < \phi < \phi_b$, but g is suitably bounded. In this case, it can be shown that if $\phi_b > q\phi_a$, the amplitude of self excited oscillations of the system is bounded by $|\phi| < q\phi_a$.

References

[1] Crocco, L., "Aspects of Combustion Stability in Liquid Propellant Rocket Motors. Part 1: Fundamentals. Low Frequency Instability with Monopropellants," *Journal of the American Rocket Society*, Vol. 21, 1951, pp. 163–178.

[2] Tsien, H. S., "Servo-Stabilization of Combustion in Rocket Motors," *Journal of the American Rocket Society*, Vol. 22, 1952, pp. 256–262.

[3] Tsien, H. S., "The Transfer Functions of Rocket Nozzles," *Journal of the American Rocket Society*, Vol. 22, 1952, pp. 139–143.

An Improved Static Probe Design

S. Z. PINCKNEY*
NASA Langley Research Center, Hampton, Va.

Introduction

PROBES for measuring in-stream static pressure in supersonic flows have been used for many years.[1] These probes have been shown to provide accurate and reliable measurement

Received October 23, 1973.

Index categories: Supersonic and Hypersonic Flow; Nozzle and Channel Flow.

* Aerospace Engineer, Hypersonic Vehicles Division.

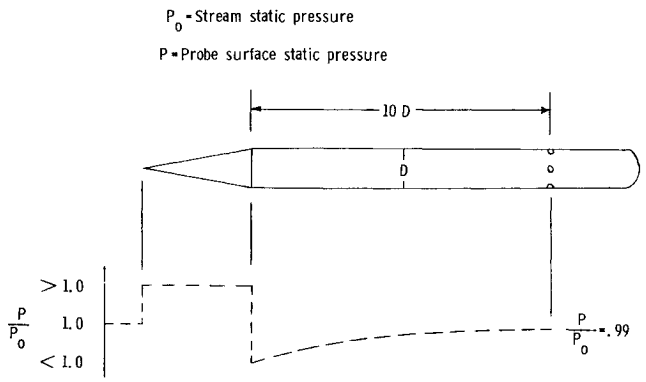

Fig. 1 Conventional static pressure probe design.

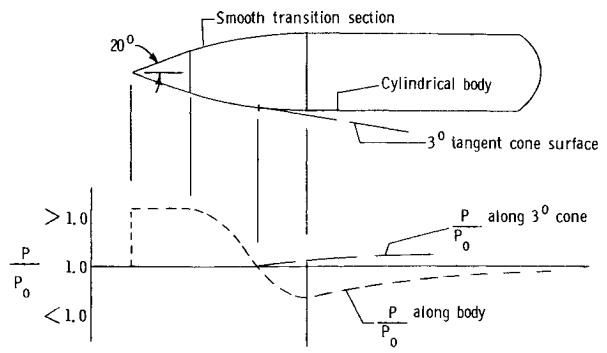

Fig. 3 Pressure distribution on faired static pressure probe.

of static pressure in large wind tunnels when aligned parallel to the flow. Figure 1 shows the shape and static pressure distribution along a conventional static probe design in which it is seen that the static holes are located approximately 10 tube diam downstream of the cone-tube shoulder where the pressure nearly equals stream static. This is typically a distance of 1 cm, or more. For the case of flow measurements in the smaller high Reynolds number facilities, however, such as in nozzle throats, inlets, and model flowfields, significant axial variations of static pressure and flow direction frequently occur in dimensions less than a centimeter. Use of a conventional probe in such cases results in the probe tip and the static holes not being in the same flow environment, and the measurement accuracy is thereby degraded.

New Probe Design

The primary constraint on the design of an improved static probe, therefore, is that the static holes be located closer to the probe tip. Note in Fig. 1, that there is a point at the shoulder of the conventional probe where static pressure falls through the freestream value, but it does so very sharply. This sharp drop can be replaced by a much more gradual change, however, by replacing the sharp shoulder with a smooth fairing between the cone and the tube. This fairing must of course be tangent to the cone and the tube at the beginning and end of the fairing, respectively, and the longer the faired section, the more gradual will be the expansion process around the shoulder. Figure 2 shows the pressure distribution on such a fairing as a function of surface slope, for two freestream Mach numbers. It is seen that the static pressure becomes equal to stream static at a surface slope of around 3° for these Mach numbers and that this slope (where $p = p_o$) is not a very sensitive function of the Mach number. If the fairing is terminated at this point and joined to a cone of about 3° half angle, then the pressure distribution will be as shown in Fig. 3, where a pressure close to stream static is maintained for a significant distance on the 3° cone section. Theoretical pressure distributions were calculated for the probe design shown in Fig. 4, which consists of a conical tip followed, respectively, by a tangent conic curve section, a tangent cone section and, finally, the cylindrical tube body. The theoretical method consisted of a blunt body program joined to a characteristics program. Results of the calculations showed that location of the static holes immediately downstream of the end of the tangent conic curve section would provide a plateau of pressure very nearly equal to stream static pressure. After construction of the probe, which was handmade for expediency, it was found that the static holes were actually located about 0.5 tube diameters downstream of the end of the conic curve section (i.e., 1.3 tube diam downstream of the projected intersection of the 20° cone and 3° conical sections).

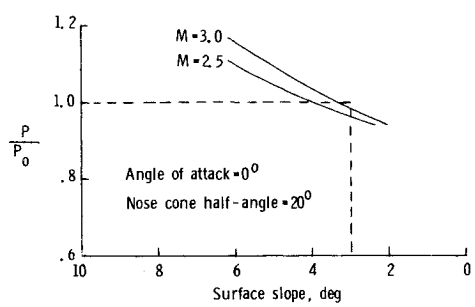

Fig. 2 Pressure distribution on faired shoulder.

Probe Tests

The new probe design shown in Fig. 4 was constructed (with a tube diameter of 0.152 cm) and tested at three freestream Mach numbers over an angle of attack range of 12°. The results are shown in Figs. 5 and 6, where p_o was measured using a conventional probe, of the same body diameter as the new probe, at zero angle of attack. It is seen in Fig. 5 that there is no significant trend of measured static pressure with angle of attack for the new probe. There is some scatter of the data seen

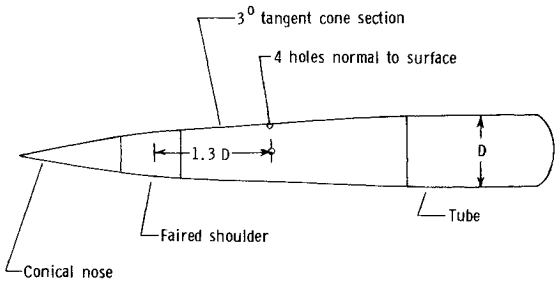

Fig. 4 Tip design of new static pressure probe.

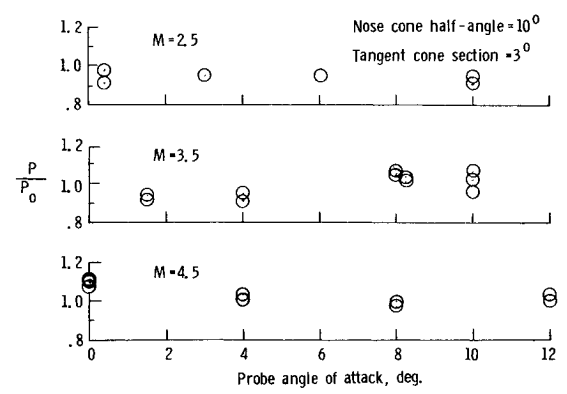

Fig. 5 Variation of measured static pressure with angle of attack.

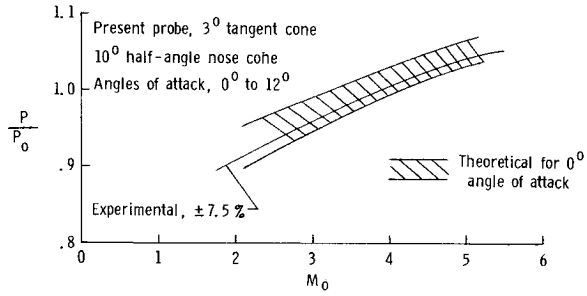

Fig. 6 Variation of measured static pressure with Mach number.

at some angles in Fig. 5 but this is not all attributable to the probe. The tunnels in which these preliminary tests were made are known to contain flow irregularities and at angle of attack, the location of the probe static holes does not exactly coincide with the point at which the reference pressure was measured. Also, since the probe was hand-made for expediency, it was not as precise as desired. The theoretical band shown in Fig. 6 is indicative of the variation in pressure due to expected changes in probe shape and static hole location resulting from construction inaccuracy. The over-all scatter in the present data, is about $\pm 7.5\%$ and this compares very favorably with conventional probes which exhibit at least 3 times this scatter under similar flow conditions. Figure 6 also shows that a given probe is fairly accurate over a reasonable range of Mach numbers; however, the probe design obviously should be tailored as closely as possible to the Mach number range of intended use, and perhaps be calibrated at several Mach numbers.

Conclusions

The new static probe design, in which the static holes are located much closer to the tip than in conventional probes, shows promise for use in certain flow situations where conventional probes become highly inaccurate. An additional advantage of the new probe design is that when used in static pressure survey rakes the probes can be located much closer together than in conventional designs and still ensure that disturbances from neighboring probe tips do not affect the static readings. A disadvantage of the new design is in the more difficult construction techniques required to provide accurately shaped tubes. However, this proved to be no great deterrent in construction of the present probes. Further study of the probe geometry is required in order to optimize the combination of cone angles, transition section length and hole location for application to any given flow situation.

References

[1] Lindsey, J. L., "Interference Effects Due to Relative Proximity of Static-Pressure Probes in Supersonic Flow," DRL-395, June 1957, University of Texas, Austin, Texas.

Flow Properties in Expansion Tube with Helium, Argon, Air, and CO_2

CHARLES G. MILLER*
NASA Langley Research Center, Hampton, Va.

Nomenclature

M_∞ = freestream Mach number
$N_{Re,\infty}$ = freestream unit Reynolds number, m^{-1}
p_∞ = freestream static pressure, kN/m^2
p_t = pitot pressure, kN/m^2
R = tube radius, m
T_∞ = freestream temperature, °K
T_t = stagnation-point temperature, °K
U_s = incident shock velocity in intermediate section, km/sec
U_∞ = freestream velocity, km/sec
y = vertical distance from tube centerline, m
Z_t = ratio of number of moles at stagnation point to number of moles of undissociated gas
ε = normal shock density ratio
ρ_∞ = freestream density, g/m^3

Received November 19, 1973.
Index categories: Nozzle and Channel Flow; Supersonic and Hypersonic Flow; Research Facilities and Instrumentation.

* Aerospace Engineer, Hypervelocity Impulse Facilities Section, Space Systems Division.

Introduction

SEVERAL studies have been performed recently in the Langley 6-in. Expansion Tube, which were unique in the sense that hypersonic and hypervelocity real-gas flows were generated with several test gases in a single facility. The capability of employing arbitrary test gases resulted in a range of normal shock density ratio (an important parameter in the simulation of real-gas effects for entry vehicles) from 4 to 19. The purpose of this Note is to present results from a calibration study performed in conjunction with these investigations. Test flow velocities from 5 to 7 km/sec were generated using helium, argon, air, and CO_2 test gases. Pitot pressure profiles across the flow at the test section are presented for the four test gases, and measured flow quantities are compared to predicted values from Ref. 1.

Apparatus and Tests

A brief description of the Langley 6-in.-Diam Expansion Tube is presented in Ref. 1. For the present tests, the driver gas was unheated helium at a nominal pressure of 33 MN/m^2 and test gases were helium, argon, air, and CO_2 at an initial pressure of 3.45 kN/m^2. For a given test, the acceleration gas was the same as the test gas, but at a lower initial pressure.

Velocities were inferred from microwave interferometer measurements and from response of pressure, heat transfer, and photomultiplier instrumentation along the length of the tube. Pressures were measured using miniature piezoelectric (quartz) transducers in conjunction with charge amplifiers. Uncertainties in measured U_s and U_∞ are believed not to exceed 4.5% and 2.5%, respectively; uncertainties in p_∞ and p_t are believed to be less than 20% and 10%, respectively.

Vertical pitot pressure profiles were made with a 9-probe survey rake positioned 4.13 cm downstream of the tube exit. Probe spacing was 1.91 cm and the o.d. of each probe, at the sensing surface, was 7.87 mm. The centerline of the center probe was coincident with the tube centerline.

Employing nominal values of measured p_∞, p_t, and U_∞ as input to the thermochemical equilibrium program of Ref. 2 yields the following calculated values in Table 1.

Table 1 Test section flow conditions

Gas	p_∞	ρ_∞	T_∞	U_∞	M_∞	$N_{Re,\infty} \times 10^{-5}$	ε	p_t	T_t	Z_t
He	1.31	2.02	305	7.04	6.82	6.63	3.76	88.9	5077	1.00
Ar	2.24	10.47	1027	5.21	8.74	9.76	7.58	268.8	13140	1.16
Air	2.14	6.97	1068	5.40	8.45	8.62	11.35	196.5	6273	1.33
CO_2	1.17	4.74	1308	5.00	9.29	5.09	18.86	116.6	3858	1.75

Results and Discussion

Vertical pitot pressure profiles are shown in Fig. 1 for the four test gases. Test repeatability, often a problem with impulse facilities, is observed to be good for helium, argon, and air, and somewhat less satisfactory for CO_2. This poorer repeatability for CO_2 is due, in part, to the difficulty of repeating and maintaining the lower value of initial acceleration gas pressure (3.1 N/m^2) required for the CO_2 tests. The profiles of Fig. 1 show the existence of a uniform test core (that is, region of uniform p_t) for all test gases. The test core diameter, defined as